Mon. Not. R. Astron. Soc. **358,** 1489–1500 (2005) doi:10.1111/j.1365-2966.2005.08875.x

Testing the locality of transport in self-gravitating accretion discs – II. The massive disc case

G. Lodato[1]★ and W. K. M. Rice[2]

[1]*Institute of Astronomy, Madingley Road, Cambridge CB3 0HA*
[2]*Institute of Geophysics and Planetary Physics, and Department of Earth Sciences, University of California, Riverside, CA 92521, USA*

Accepted 2005 January 26. Received 2005 January 24; in original form 2004 November 24

ABSTRACT

In this paper, we extend our previous analysis (Paper I) of the transport properties induced by gravitational instabilities in cooling, gaseous accretion discs to the case where the disc mass is comparable to the central object. In order to do so, we have performed global, three-dimensional smoothed particle hydrodynamics simulations of massive discs. These new simulations show a much more complex temporal evolution with respect to the less massive case. Whereas in the case of low disc mass a self-regulated, marginally stable state (characterized by an approximately constant radial profile of the stability parameter Q) is easily established, in the case of high disc mass we observe the development of an initial transient and subsequent settling down in a self-regulated state in some simulations, or a series or recurrent spiral episodes, with low azimuthal wavenumber m, in others. Accretion in this last case can therefore be a highly variable process. On the other hand, we find that the secular evolution of the disc is relatively slow. In fact, the time average of the stress induced by self-gravity results in accretion time-scales much longer than the dynamical time-scale, in contrast with previous isothermal simulations of massive accretion discs. We have also compared the resulting stress tensor with the expectations based on a local theory of transport, finding no significant evidence for global wave energy transport.

Key words: accretion, accretion discs – gravitation – instabilities – stars: formation – galaxies: active – galaxies: spiral.

1 INTRODUCTION

It is now becoming progressively more clear (from both the theoretical and the observational points of view) that gravitational instabilities might play an important role in the dynamics of accretion discs, both on the large scales of active galactic nuclei (AGN) and on the small scales of protostellar and protoplanetary discs.

At the AGN scale, a powerful observational tool is provided by water maser observations of the gas motions at distances of $\approx$1 pc from the central black hole (Greenhill & Gwinn 1997; Kondratko et al. 2005), which often show that the rotation curve can depart significantly from a Keplerian profile, suggesting that the disc itself might give a significant contribution to the gravitational field. Indeed, in the case of the Seyfert galaxy NGC 1068, simple self-gravitating disc models are able to reproduce the observed non-Keplerian rotation curve (Lodato & Bertin 2003a).

The case for self-gravitating accretion discs is perhaps even stronger in the context of star and planet formation. It has long been argued (Lin & Pringle 1987) that in the early stages of star formation the disc mass can be sufficiently high for the effect of its self-gravity to become important. Simple estimates by Larson (1984) led to the conclusion that a gravitationally unstable disc is a likely outcome of the isothermal collapse of protostellar clouds. The recent discovery of a 100 $M_\odot$ disc surrounding a massive (20 $M_\odot$) protostar in the M17 nebula (Chini et al. 2004) would clearly indicate, if the mass estimates are confirmed, that the formation of a massive star undergoes a phase of self-gravitating disc accretion. In the case of low-mass (proto)stars, disc mass estimates are uncertain, but discs in the upper end of the mass distribution for T Tauri stars (Launhardt & Sargent 2001; Natta et al. 2004) can have a mass $\approx$30 per cent of that of the central star. In addition, there have also been theoretical suggestions that the disc self-gravity might be important in the outer disc of FU Orionis objects (Bell & Lin 1994; Armitage, Livio & Pringle 2001; Lodato & Bertin 2003b).

Recently, the disc self-gravity has been considered especially in view of the possibility of forming smaller-mass companions by the direct fragmentation of a gravitationally unstable disc, with obvious implications for the formation of gas giant planets in a protostellar disc [see, for example, Boss (2002) and Rice et al. (2003c) or, for similar arguments on the galactic scale, Goodman & Tan (2004)]. However, it has now become clear that the outcome of gravitational

★E-mail: giuseppe@ast.cam.ac.uk

© 2005 RAS

instabilities strongly depends on the thermodynamics of the disc. In particular, the fragmentation of a gravitationally unstable disc requires that the disc be able to cool very efficiently (Gammie 2001; Rice et al. 2003a), with a cooling rate $t_{\rm cool} \lesssim 3\Omega^{-1}$ (where Ω is the angular velocity of the disc). This is a rather severe requirement for a protostellar disc, so that the formation of planets from the direct fragmentation of a massive disc seems rather unlikely [however, the inclusion of the effects of convection might substantially reduce the cooling time-scale – see Boss (2004a)]. In any case, even the simple development of a gravitational instability in the form of a spiral structure can significantly accelerate the process of planet formation by favouring the agglomeration of planetesimals (Haghighipour & Boss 2003; Rice et al. 2004). Moreover, gravitational stresses might play another important role in the process of planet formation, since the mixing induced by these stresses can influence the early evolution of chemical elements in protoplanetary discs (Boss 2004b).

Another important issue related to the disc self-gravity is its ability to transport angular momentum and thus to promote the process of accretion. This has been recognized in the analysis of isothermal simulations of massive discs (Laughlin & Bodenheimer 1994; Laughlin & Ròżyczka 1996) and subsequently analysed in a number of papers (Pickett et al. 1998, 2000; Nelson et al. 2000). However, only recently have simulations been performed that include a relatively more complex treatment of the thermal status of the disc (Rice et al. 2003a; Pickett et al. 2003; Mejia et al. 2005). In a previous paper (Lodato & Rice 2004, hereafter Paper I), we have explored in detail the transport properties of self-gravitating, cooling discs, by performing some high-resolution smoothed particle hydrodynamics (SPH) simulations. These simulations were used to explore the extent to which angular momentum and energy transport via gravitational instability can be regarded as a local phenomenon, or whether the intrinsic global nature of the instabilities would preclude such an approach. The simulations described in Paper I included disc masses up to $0.25\,M_\star$ (where $M_\star$ is the mass of the central object) and showed how, when the disc is allowed to cool down due to external cooling and to heat up as a consequence of the development of gravitational spiral instabilities, it eventually settles down in a marginally stable state, characterized by an approximately flat profile of the parameter Q:

$$Q = \frac{c_{\rm s}\kappa}{\pi G \Sigma} \approx 1, \tag{1}$$

where $c_{\rm s}$ is the thermal speed, κ is the epicyclic frequency and Σ is the surface density of the disc. The resulting spiral structure turned out to be a quasi-stationary structure, evolving only on the long 'viscous' time-scale, and able to transport angular momentum and energy at a rate which is in reasonable agreement with the expectations based on a local (viscous) theory of transport.

It can be shown that, for self-regulated discs, a simple relationship holds between the disc aspect ratio H/R and the mass ratio $M_{\rm disc}/M_\star$. The disc is in fact marginally stable when its temperature is small enough that $H/R \lesssim M_{\rm disc}/M_\star$. Of course, this relationship can only hold in the limit where $M_{\rm disc}/M_\star \ll 1$. As $M_{\rm disc}/M_\star$ grows, the disc becomes thicker, and global effects are going to be more important. This was already shown by us in Paper I. The limit $M_{\rm disc}/M_\star \sim 1$ is therefore particularly interesting, because we expect a different physics to come into play.

In this paper we extend our previous analysis, considering the case where the disc mass is particularly high. We have in fact considered the two cases where $M_{\rm disc} = 0.5\,M_\star$ and $M_{\rm disc} = 1\,M_\star$. The results of these new simulations present significant differences with respect to our previous analysis. In the case of high disc mass, we now find the development of transient, global spiral structures, which last for roughly one dynamical time-scale and develop recurrently during the course of the simulation. While in the $M_{\rm disc} = 0.5\,M_\star$ case, after a first transient, the disc is eventually able to settle down in a quasi-stationary state, in the equal-mass case the disc is not able to 'self-regulate' the strength of the spiral disturbance in order to counterbalance exactly the externally imposed cooling and short-lived global disturbances recurrently develop during the whole simulation. Accretion in this last case will therefore appear to be a highly variable process.

The paper is organized as follows. In Section 2 we briefly review the relevant physical concepts of the problem and the details of the numerical setup that we adopt. In Section 3 we describe the results of our simulations. In Section 4 we discuss our results and draw our conclusions.

2 BASIC CONCEPTS AND NUMERICAL SETUP

2.1 Basic physical quantities

In this section we briefly review the basic concepts about the evolution of viscous discs and the development of gravitational instabilities and their associated transport properties. More details can be found in section 2 of Paper I and references therein.

The equations of motion for an axisymmetric disc, in cylindrical coordinates, are the equation of continuity,

$$\frac{\partial \Sigma}{\partial t} + \frac{1}{R}\frac{\partial}{\partial R}(R\Sigma u) = 0, \tag{2}$$

and the azimuthal component of Euler's equation (expressed in terms of angular momentum conservation),

$$\frac{\partial}{\partial t}(\Sigma R^2 \Omega) + \frac{1}{R}\frac{\partial}{\partial R}(\Sigma R^3 \Omega u) = -\frac{1}{R}\frac{\partial}{\partial R}\left(R^2 T_{R\phi}\right), \tag{3}$$

where u is the radial velocity and $T_{R\phi}$ is the relevant component of the viscous stress tensor, integrated in the vertical direction. This last term is the basic ingredient in the theory of accretion discs. Standard hydrodynamical viscosity is not sufficient to provide accretion at the required rates, and therefore $T_{R\phi}$ is generally described by means of ad hoc prescriptions. The α prescription (Shakura & Sunyaev 1973), based on simple arguments on the relevant physical scales of turbulent cells in the discs, assumes that $T_{R\phi}$ is proportional to the disc pressure,

$$T_{R\phi} = \left|\frac{{\rm d}\ln\Omega}{{\rm d}\ln R}\right| \alpha \Sigma c_{\rm s}^2, \tag{4}$$

where the proportionality constant α is an unknown parameter, usually considered to be smaller than unity. The α prescription can also be put in the following equivalent form, which involves the kinematical viscosity coefficient ν,

$$\nu = \alpha c_{\rm s} H, \tag{5}$$

where H is the thickness of the disc.

The effect of viscosity on the energy balance is two-fold: viscous torques convect energy between neighbouring annuli of the disc and they dissipate energy. The energy that is convected across a ring at radius R per unit time is given by

$$\frac{{\rm d}E}{{\rm d}t} = 2\pi R^2 T_{R\phi}\Omega, \tag{6}$$

while the dissipation rate per unit surface is given by

$$D(R) = T_{R\phi}|R\Omega'|. \tag{7}$$

If the disc is in thermal equilibrium, we can derive a useful relation between the viscosity coefficient α and the cooling time-scale. If we assume that cooling can be simply parametrized as

$$Q^- = \frac{U}{t_{\rm cool}} = \frac{\Sigma c_{\rm s}^2}{\gamma(\gamma-1)t_{\rm cool}}, \tag{8}$$

where U is the internal energy per unit surface and γ is the ratio of the specific heats, then, equating the viscous dissipation term, expressed in equation (7), to the cooling term, expressed in equation (8), leads to

$$\alpha = \left|\frac{{\rm d}\ln\Omega}{{\rm d}\ln R}\right|^{-2} \frac{1}{\gamma(\gamma-1)t_{\rm cool}\Omega}, \tag{9}$$

where we have used also equation (4).

2.2 Diagnostics for gravitationally induced transport

In order to describe the development and the properties of a self-gravitating structure, we will use the same diagnostics adopted in Paper I, and we summarize them here.

The basic parameter that describes the local, axisymmetric stability of a gaseous disc with respect to gravitational instabilities is the Q parameter defined in equation (1). It actually turns out that the stability criterion based on this parameter, namely that $Q \gtrsim 1$, is quite robust, and generally applicable also in the case of global, non-axisymmetric disturbances (see also Paper I). As mentioned in the Introduction, and as discussed in more details elsewhere (Paczyński 1978; Bertin 1997; Paper I), the competitive effects of external cooling and effective heating due to gravitational instabilities tend to result in a self-regulated state, where the value of Q is constant throughout the disc and very close to its marginal stability value. The simulations presented in Paper I confirmed the effectiveness of the self-regulation mechanism. We will therefore track the development of a self-regulated state by looking at the profile of Q.

The relevant component of the stress tensor associated with gravitational instabilities is defined as (Lynden-Bell & Kalnajs 1972)

$$T_{R\phi}^{\rm grav} = \int {\rm d}z\, \frac{g_R g_\phi}{4\pi G}, \tag{10}$$

where g_R and g_ϕ are the radial and azimuthal components of the gravitational field, respectively. The full stress tensor also includes the 'Reynolds' stress, defined as

$$T_{R\phi}^{\rm Reyn} = \Sigma \delta v_R \delta v_\phi, \tag{11}$$

where $\delta\boldsymbol{v} = \boldsymbol{v} - \boldsymbol{u}$, with $\boldsymbol{v}$ the fluid velocity and $\boldsymbol{u}$ the mean fluid velocity. It is always possible to define an effective α parameter associated with gravitational instabilities, by setting

$$T_{R\phi}^{\rm grav} + T_{R\phi}^{\rm Reyn} = \left|\frac{{\rm d}\ln\Omega}{{\rm d}\ln R}\right| \alpha \Sigma c_{\rm s}^2. \tag{12}$$

A local description of angular momentum transport then requires that the stress tensor, and therefore α, at a given location is only determined by local conditions in the disc. In Paper I we have already shown that in self-gravitating discs a region of size $\approx 10H$ contributes to the stress at a given location, therefore implying that, for discs as thick as $H/R \approx 0.1$, the stress tensor is not determined locally.

In addition, there is also another issue concerning the use of a viscous formalism in self-gravitating accretion discs. In fact, Balbus & Papaloizou (1999) have shown that in general the energy transport provided by gravitational instabilities contains global terms, associated with wave energy transport, which cannot be directly associated with an effective viscosity. It remains to be discussed how large these terms are, and under which conditions they play a significant role. Balbus & Papaloizou (1999) argue that global energy transport should not play an important role in a marginally stable disc. In this case, a viscous description of transport should be appropriate and therefore energy should be transported according to equation (6) and it should be dissipated according to equation (7). If the disc is in thermal equilibrium, the latter statement is equivalent to the prescription that α and $t_{\rm cool}$ are related through equation (9). This offers us a simple test to check whether energy dissipation is actually viscous or not in massive discs. In particular, since in all our simulations (as discussed below), we adopt $\gamma = 5/3$ and $t_{\rm cool} = 7.5\Omega^{-1}$, the expected value of α for viscous dissipation to balance cooling is $\alpha \approx 0.053$.

2.3 Numerical issues and setup

The numerical setup is largely identical to that used in Paper I. We use smoothed particle hydrodynamics (SPH) (see Benz 1990; Monaghan 1992) to perform three-dimensional simulations of gaseous accretion discs. We consider a system comprising a central star, with mass $M_\star$, surrounded by a disc, with mass $M_{\rm disc}$, and we consider mass ratios $q = M_{\rm disc}/M_\star$ of 0.5 and 1. The disc is modelled using 250 000 SPH particles, while the central object is modelled as a point mass on to which gas particles may accrete if they move to within the accretion radius. Both the gas particles and the point mass use a tree to determine neighbours and to calculate gravitational forces (Benz 1990), and the central object is free to move under the gravitational influence of the disc gas.

The disc particles are distributed such as to give an initial surface density profile of $\Sigma \propto R^{-1}$ with an initial temperature profile chosen to be $T \propto R^{-1/2}$. The initial velocity profile is calculated by including the enclosed mass and the pressure gradient when determining the angular frequency Ω. With these initial conditions, the minimum value of Q is attained at the outer edge of the disc. For each simulation, the temperature normalization is chosen such that the minimum value of Q is $Q_{\rm min} = 2$, giving a disc that is initially gravitationally stable. The disc is also assumed to be in vertical hydrostatic equilibrium (see, for example, Pringle 1981). The particles are therefore distributed such that the vertical density profile is a Gaussian with a scaleheight H given by $H = c_{\rm s}/\Omega$. Actually, in a self-gravitating disc, the vertical density profile is not rigorously Gaussian (Bertin & Lodato 1999; Huré 2000), so our initial setup, strictly speaking, is not in dynamical equilibrium. However, dynamical equilibrium is achieved rapidly (i.e. in a dynamical time-scale) during the simulation.

Our calculations are essentially scale-free. In dimensionless units, the disc extends from $R_{\rm in} = 0.25$ to $R_{\rm out} = 25$ and the star has a mass of $M_\star = 1$. In these units, the orbital period at $R = 1$ is 2π code units and one orbital period at the outer edge of the disc is approximately 800 time units.

Since the main aim of this work, as in Paper I, is to investigate transport properties of self-gravitating accretion discs, we explicitly solve the energy balance for the gas. We allow the disc to heat up due to both $P\,{\rm d}V$ work and viscous dissipation, and assume that the ratio of the specific heats is $\gamma = 5/3$. We then impose a cooling of the form (Gammie 2001)

$$\frac{{\rm d}u_{\rm i}}{{\rm d}t} = -\frac{u_{\rm i}}{t_{\rm cool}}, \tag{13}$$

where $u_{\rm i}$ is the internal energy per unit mass and $t_{\rm cool}$ is given by $t_{\rm cool} = \beta\Omega^{-1}$. Previous simulations (Gammie 2001; Rice et al.

2003b) have shown that discs fragment for $\beta \leqslant 3$, with this fragmentation boundary possibly increasing as the disc mass increases (Rice et al. 2003b). To ensure that our discs do not fragment, we use $\beta = 7.5$. The imposed cooling should lead to the growth of the gravitational instability, which will heat the disc, returning it to a state of marginal stability. There will also be additional heating through the artificial SPH viscosity. In these simulations we use the standard SPH viscosity (e.g. Monaghan 1992) but also include the Balsara switch (Balsara 1995) to reduce the shear component of the artificial viscosity. As discussed in detail in Paper I, the angular momentum transport induced by the artificial viscosity is at least a factor of 10 smaller than that due to the gravitational instabilities. The artificial viscosity should therefore play only a minor role in the disc dynamics.

3 RESULTS

In this section we describe the main results of our simulations. As mentioned above, all the simulations are scale-free and can therefore describe the basic dynamics of different astrophysical systems (from protostellar discs to AGN discs or even to galactic discs), even if we do not intend to model the detailed physical appearance of a specific one. However, when numbers are needed, we will consider as a reference case, for illustrative purposes, a 'low-mass protostar circumstellar disc', where the central object mass is 1 $M_\odot$ and the unit length of the simulations is $R_0 = 1$ AU. Thus, in this reference case, the disc extends from $R_{\rm in} = 0.25$ AU to $R_{\rm out} = 25$ AU. We will express all times in units of the *Keplerian* rotation period of the outer disc $t_0 = 2\pi/\Omega_{\rm out}$, where $\Omega^2_{\rm out} = GM_\star/R^3_{\rm out}$. For most cases, we have followed the simulations up to $\approx 7t_0$, i.e. up to a few thermal time-scales at the outer edge of the disc.

3.1 The $M_{\rm disc} = 0.5\,M_\star$ case

The evolution of the disc in this case is characterized by two phases: (i) soon after the beginning of the simulation, the disc develops a large-scale, transient spiral structure that subsequently vanishes; (ii) at later times, the disc settles down in a quasi-stationary state, characterized by a much slower evolution. Here we describe the two stages separately.

3.1.1 The initial transient

In the earliest stages of the simulation, the disc simply cools down, until (at roughly $t = 2t_0$) the minimum value of Q approaches unity and the first gravitational disturbances start to develop. These are dominated by a grand-design, $m = 2$ spiral mode. The pattern frequency of this mode (i.e. the angular velocity of a reference frame in which the spiral is stationary) is $\Omega_{\rm p} \approx 1.5\Omega_{\rm out}$. In this case the corotation radius (i.e. the radius at which the spiral mode and the gas rotate with the same angular velocity) is $R \approx 19$, very close to the outer edge of the disc. This large-scale structure is, however, not long-lived, and has essentially disappeared at $t \approx 3t_0$ (i.e. after one dynamical time-scale), leaving behind a smaller-scale disturbance characterized by modes with larger m and confined within the inner disc. Fig. 1 shows the logarithm of the disc surface density (with a colour scale ranging between 10^4 and 10^7 g cm^{-2}) during the development of this transient disturbance. The four images refer to $t = 0,\ 1.9t_0,\ 2.5t_0$ and $3t_0$, respectively. The linear scale of the images ranges between -25 and 25 for both axes.

The development of this spiral is accompanied by a significant modification of the profile of Q. Fig. 2 shows the Q profile at $t = 1.9t_0$ (solid line), $t = 2.7t_0$ (dotted line) and, for comparison, at $t = 7t_0$, i.e. at the end of the simulation, when a self-regulated state is eventually achieved (dashed line). It can be seen that this first spiral transient leads to a strong 'heating' of the outer disc, with Q rising well above unity. In this way the outer disc is stabilized and the large-scale spiral structure rapidly vanishes.

Another important feature associated with this transient spiral instability is the mass transport induced by it. We have evaluated the strength of the torques excited by the gravitational instability as discussed in Section 2. The left panel of Fig. 3 shows the evolution of the parameter α at four different times during the transient: $t = 2.28t_0$ (solid line), $t = 2.52t_0$ (short-dashed line), $t = 2.69t_0$ (long-dashed line) and $t = 2.93t_0$ (dot-dashed line). The two horizontal dotted lines show the expected 'equilibrium' value $\alpha = 0.053$, obtained from balancing viscous heating and cooling (as discussed above in Section 2), and the maximum torque strength ($\alpha = 0.005$) due to artificial SPH viscosity (see Paper I, appendix). It is apparent that the transient induces a strong angular momentum transport in the outer disc, with maximum values of α rising above 0.2. At later times, when the transient vanishes, the value of α decreases accordingly, becoming much smaller than 0.053 in the outer disc, and close to 0.053 within $R = 5$. The right panel of Fig. 3 shows the corresponding mass accretion rates (if we use the scale units of the reference case). The $\dot{M}$ induced by the transient is significant in the outer disc, becoming as large as $\approx 10^{-4}\,{\rm M}_\odot\,{\rm yr}^{-1}$, and then decreasing significantly once the transient has disappeared.

The large mass accretion rate of course induces a significant redistribution of matter in the disc. This is shown in Fig. 4, where we plot the azimuthally averaged surface density of the disc at $t = 0$ (solid line) and at $t = 2.93t_0$ (dotted line). The spiral structure has produced a steepening of the surface density profile.

Bertin & Lodato (1999) have studied a class of steady-state, self-regulated massive accretion disc models. The surface density profile of these models asymptotically approaches $\Sigma \sim r^{-1}$ at large radii, but it shows significant departures from a simple power law at small radii, becoming progressively steeper. These self-regulated models depend on only one dimensional parameter: a scalelength $R_{\rm s}$, defined as

$$R_{\rm s} = 2GM_\star \left(\frac{\bar{Q}}{4}\right)^2 \left(\frac{G\dot{M}}{3\alpha}\right)^{-2/3}, \qquad (14)$$

where $\bar{Q} \approx 1$ is the marginally stable value of Q. The dashed line in Fig. 4 shows the surface density profile of this analytical model, with $R_{\rm s} = 200$ AU. With this choice, the mass enclosed within 25 AU is $0.5\,M_\star$, i.e. the same as in our simulation. This density profile matches well the surface density profile obtained after the occurrence of the transient spiral. This suggests that this episode of gravitational instability is the response of the disc to the initial conditions assumed here. The disc's 'preferred' state is a self-regulated state, in which the surface density profile is slightly steeper than the initial $\Sigma \propto R^{-1}$. The large-scale spiral transient that we observe has the effect of moving just enough matter so as to steepen the surface density profile to match the one implied by the self-regulation condition.

3.1.2 Long-term evolution

After the first transient, the value of Q in the outer disc is relatively high (see Fig. 2) and the spiral structure is confined to the inner disc. In this way, the main source of heating in the outer disc (i.e. the effective heating due to gravitational instabilities) is turned off

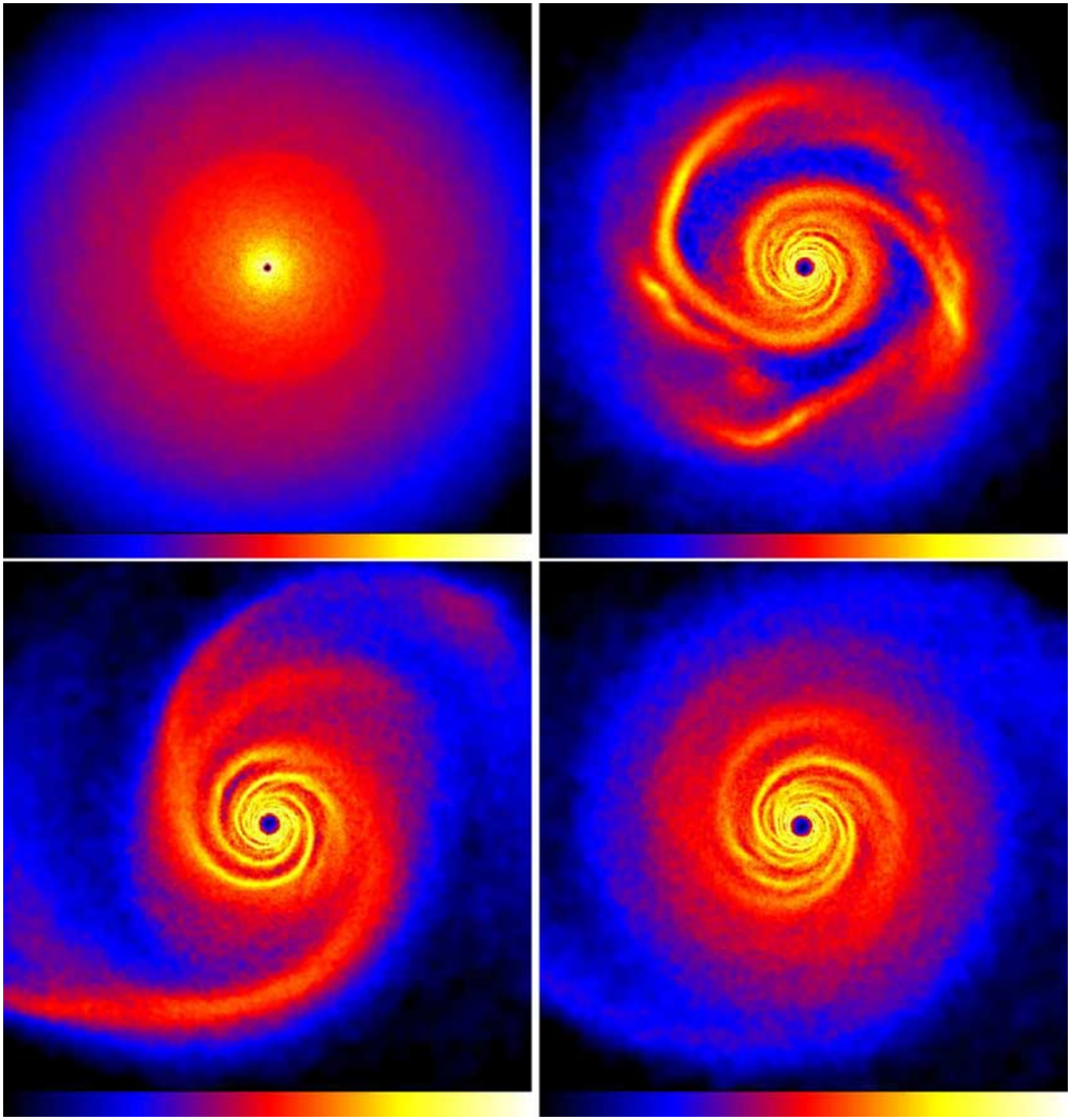

Figure 1. Time evolution of the logarithm of the surface density Σ (with a colour scale ranging between 10^4 and 10^7 g cm^{-2}) during the development of the transient spiral structure at the beginning of the $M_{\rm disc} = 0.5\,M_\star$ simulation. They refer to $t = 0$ (upper left), $t \approx 1.9\,t_0$ (upper right), $t \approx 2.5\,t_0$ (lower left) and $t \approx 3t_0$ (lower right). The linear scale of the images ranges from -25 to 25 (in code units) for both axes.

and the disc cools down until a new generation of gravitational disturbances eventually develops. Fig. 5 shows the surface density of the disc at the end of the simulation. The scales are exactly the same as in Fig. 1.

This second episode of gravitational instability is, however, different in nature to the previous one. It is not transient, but lasts for several outer dynamical time-scales (from $t \approx 4t_0$ until at least the end of the simulation, at $t = 7t_0$), showing no significant evolution throughout. This can be seen in Fig. 6, which shows the profile of Q at $t = 5.2t_0$ (solid line), $t = 5.8t_0$ (dotted line) and $t = 6.6t_0$ (dashed line) (for comparison, see the evolution shown in Fig. 2). Fig. 7 shows the amplitude of the first 15 Fourier components of the density structure at the end of the simulations, computed as in Paper I. It can be seen that the disc is dominated by low-m modes, with $m \lesssim 5$, even if it does not show a clear two-armed structure as during the first transient phase.

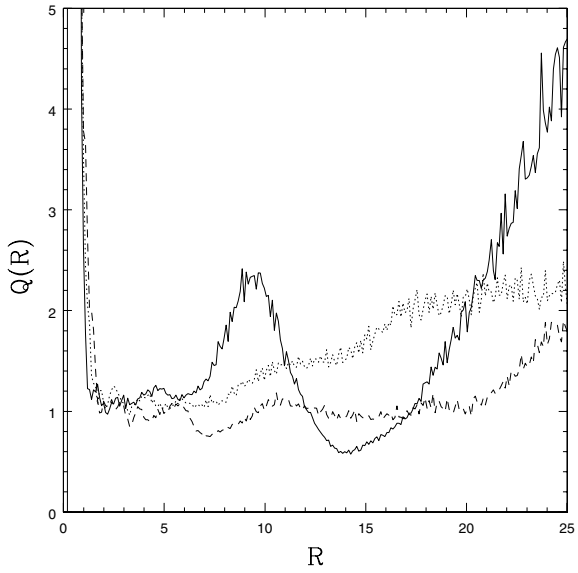

Figure 2. Evolution of the profile of Q during the transient in the $M_{\rm disc} = 0.5\,M_\star$ simulation. The three curves refer to $t = 1.9t_0$ (solid line), $t = 2.7t_0$ (dotted line) and $t = 7t_0$ (dashed line).

In order to discuss the transport properties associated with this quasi-stationary structure, we have computed the stress tensor averaged over 640 time units, i.e $\approx 0.8t_0$. The results are shown in Figs 8 and 9. The bottom panel of Fig. 8 shows the average stress tensor, as measured by the α parameter (solid line), and the expected value of α obtained by imposing that the viscous heating rate exactly balances the cooling rate (dotted line). There is substantial agreement between the two values. The lower dotted line shows, as in the left panel of Fig. 3, the maximum contribution to the stress coming from artificial SPH viscosity. The upper panel of Fig. 8 shows a comparison between the cooling rate (dashed line) and $D(R)$, the viscous heating rate (solid line), defined in equation (7). Again, there is a substantial agreement between the two, suggesting that, even for this relatively massive disc, a state of thermal equilibrium has been reached and that the energy dissipation process is well described by a simple viscous model.

In Fig. 9 we plot the radial profiles of $\dot{M}$ (upper panel) and of $t_\nu/t_{\rm K}$ (lower panel), where $t_\nu = R^2/\nu$ is the viscous time-scale and $t_{\rm K} = \Omega_{\rm K}^{-1}$ is a measure of the dynamical time-scale. We see that the mass accretion rate acquires an almost constant value, consistent with the quasi-stationary character of the spiral structure, with $\dot{M} \approx 2 \times 10^{-5}$ M$_\odot$ yr^{-1}. Note that, even if the value of α is not particularly high, the mass accretion rate is conspicuous since the disc is relatively hot. However, despite the high $\dot{M}$, the inspection of the bottom panel of Fig. 9 shows that accretion occurs on a long time-scale, more than three orders of magnitude larger than the dynamical time-scale.

3.2 The $M_{\rm disc} = 1\,M_\star$ case

In this case, the initial evolution of the disc is similar to that observed in the other simulations. The disc initially simply cools down until Q becomes of the order of unity in the inner disc (where the cooling time is fastest) and gravitational instabilities set in. However, the long-term evolution of this massive disc differs from the long-term evolution of the lower-mass discs. A relatively small-amplitude spiral structure, confined within $R \approx 15$, is always present once the disc has cooled down sufficiently. However, a series of recurrent, prominent large-scale spiral disturbances occur repeatedly throughout the course of the simulation. The amplitude of the $m = 2$ Fourier component, in the outer disc, is plotted as a function of time in Fig. 10. Major episodes of spiral activity can be easily recognized at $t \approx 1.5t_0$, $4t_0$ and $6t_0$. A similar cyclic behaviour, with a modulation of the amplitude of the dominant $m = 2$ mode, has been found in previous simulations of self-gravitating discs (Sellwood & Carlberg 1984; Laughlin & Bodenheimer 1994; Laughlin, Korchagin & Adams 1998). Laughlin et al. have attributed this behaviour to the effect of non-linear coupling between different modes.

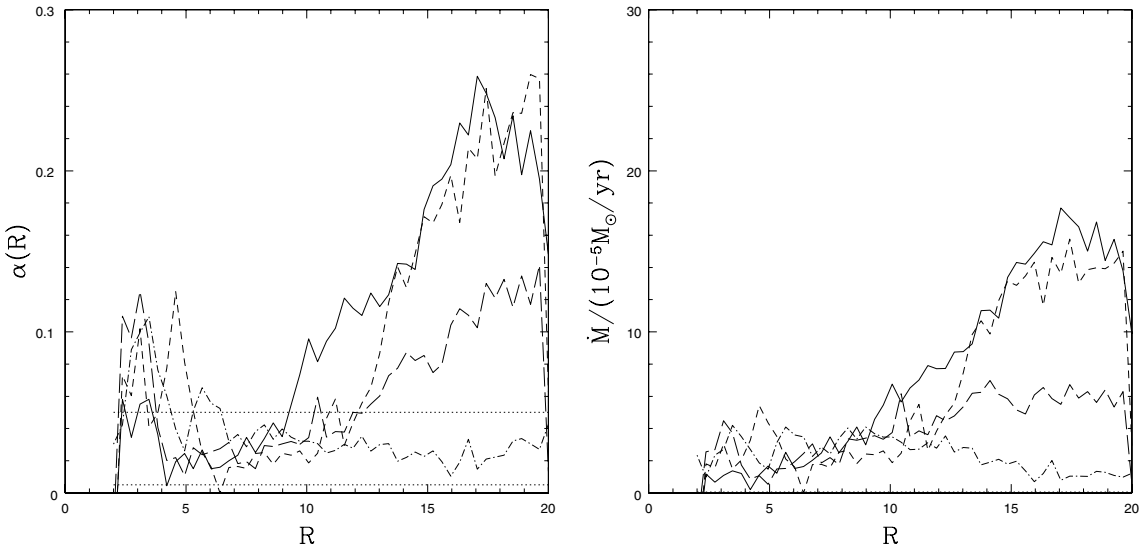

Figure 3. Left: Evolution of the gravitational torque strength (as measured by the dimensionless parameter α) during the transient. The four lines refer to $t = 2.28t_0$ (solid line), $t = 2.52t_0$ (short-dashed line), $t = 2.69t_0$ (long-dashed line) and $t = 2.93t_0$ (dot-dashed line). The two horizontal dotted lines show the expected 'equilibrium' value $\alpha = 0.053$, obtained from balancing viscous heating and cooling, and the maximum torque strength ($\alpha = 0.005$) due to artificial SPH viscosity (see Paper I, appendix). Right: Corresponding mass accretion rates, assuming that the central object is 1 M$_\odot$ and that the unit length is 1 AU.

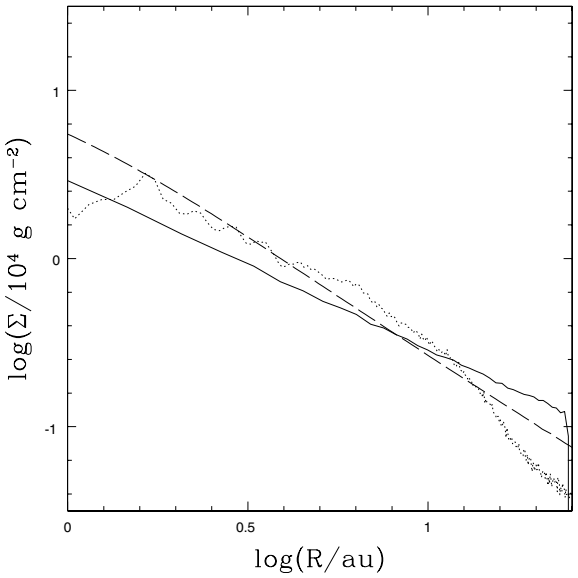

Figure 4. Azimuthally averaged surface density profiles at $t = 0$ (solid line) and $t = 2.93t_0$ (dotted line). The dashed line shows the surface density profile predicted by the self-regulated disc models of Bertin & Lodato (1999).

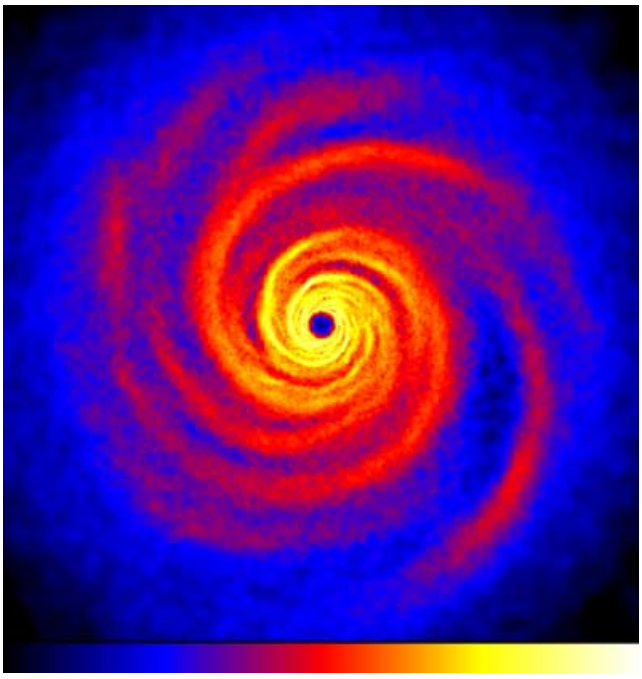

Figure 5. Surface density in the $M_{\rm disc} = 0.5\,M_\star$ case, at the end of the simulation. The scales are the same as in Fig. 1.

3.2.1 *The large-scale spiral*

Because all the large-scale spiral disturbances share a similar physical appearance, we will describe, as an example, one such episode, which developed at $t \approx 5.8t_0$ and has vanished by $t \approx 6.5t_0$. The structure of the disc at $t \approx 5.9t_0$ is shown in the left panel of Fig. 11 (for comparison, the right panel shows the structure at $t \approx 3t_0$, during a period of low spiral activity; see Fig. 10). The disc is clearly dominated by a large-scale $m = 2$ mode, with a pattern frequency $\Omega_{\rm p} \approx 3\Omega_{\rm out}$, resulting in corotation at $R \approx 14$. Fig. 12 shows the

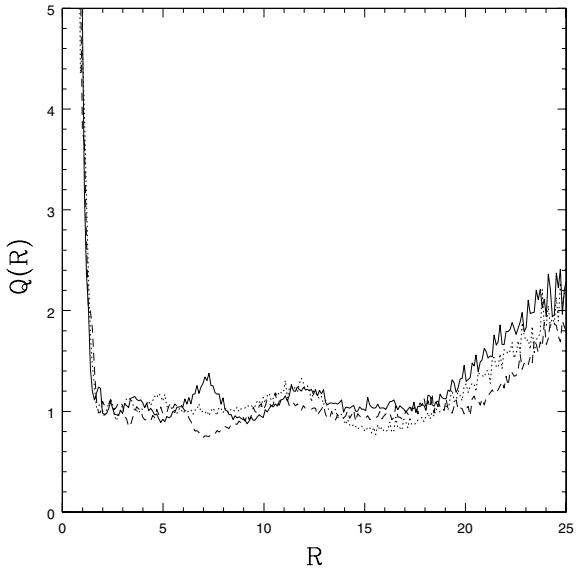

Figure 6. Profiles of Q at $t = 5.2t_0$ (solid line), $t = 5.8t_0$ (dotted line) and $t = 6.6t_0$ (dashed line).

evolution of the profile of Q (left) and of the azimuthally averaged surface density Σ (right) during the development of the spiral structure. The curves refer to $t \approx 5.4t_0$ (before the onset of the instability; solid line), $t \approx 5.9t_0$ (during the disturbance; dotted line), and at $t \approx 6.5t_0$ (after the spiral episode has vanished; dashed line). Before the spiral develops, the disc is characterized by a flat, self-regulated, Q profile out to $R \approx 17$. Therefore, it appears that the corotation of the spiral mode occurs close to the outer edge of the self-regulated portion of the disc. Note that the inner Lindblad resonance (ILR) for this mode occurs at $R \approx 5$, and does not influence the propagation of the density wave to small radii, in our hydrodynamical simulations. On the other hand, it is well known that, for a stellar (collisionless) disc, waves are efficiently absorbed at the ILR.

The effect of the development of the spiral is to remove angular momentum from inside corotation and to release it to the matter located outside corotation. As a result, outside corotation the disc expands and its surface density decreases. This is evidenced from the appearance of a local minimum in the surface density at corotation (dotted line in the right panel of Fig. 12), which corresponds to a local maximum in the Q profile. After the spiral has vanished, the Q profile is very similar to before the onset of the transient structure, with the self-regulated part of the disc extending out to a slightly smaller radius.

3.2.2 *Secular evolution*

As mentioned above, the appearance of a grand-design $m = 2$ mode gives rise to a substantial angular momentum transport over a small period of time (namely, the duration of the $m = 2$ disturbance). We have computed the time average of the effective α produced by the gravitational instabilities at two different times during the evolution of the disc: (i) between $t = 2.7t_0$ and $3.5t_0$, during which period no dominant large-scale structure was observed, and (ii) between $t = 5.8t_0$ and $6.6t_0$, i.e. during the development of a large-scale spiral structure (see also Fig. 10). The results are shown in Fig. 13, where $\alpha(R)$ is shown during low spiral activity (solid line) and high spiral activity (dashed line). During high spiral activity the gravitational torques are larger, but not by a particularly significant amount. During both periods the value of α lies very close to the

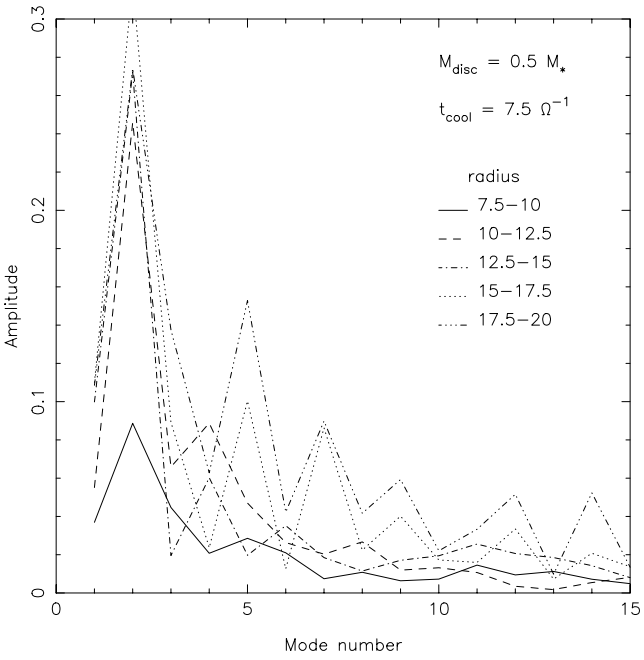

Figure 7. Amplitude of the first Fourier components of the density structure in the $M_{\rm disc} = 0.5\,M_\star$ case for different radial ranges in the disc.

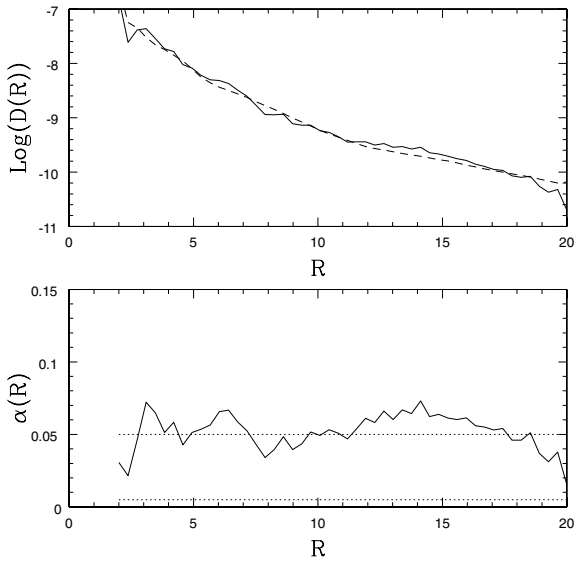

Figure 8. Bottom: Effective α produced by gravitational instabilities in the $M_{\rm disc} = 0.5\,M_\star$ case (solid line); and value of α expected from balancing viscous heating and external cooling (upper dotted line). The lower dotted line shows the maximum contribution to the stress given by artificial viscosity in SPH, as in Fig. 4. Top: Viscous heating power $D(R)$ (solid line) compared to externally imposed cooling (dashed line).

expectation based on a balance between viscous heating and cooling. If the reference numerical values for the relevant scales are used (1 $M_\odot$ for the unit mass and 1 AU for the unit length), the accretion rate would be of the order of $\dot{M} \approx 10^{-4}$ $M_\odot$ yr^{-1}. The accretion time-scale is still very large compared to the dynamical time ($t_\nu/t_{\rm K} \approx 10^3$), and has a very weak dependence on radius, as in the case where $M_{\rm disc} = 0.5\,M_\star$.

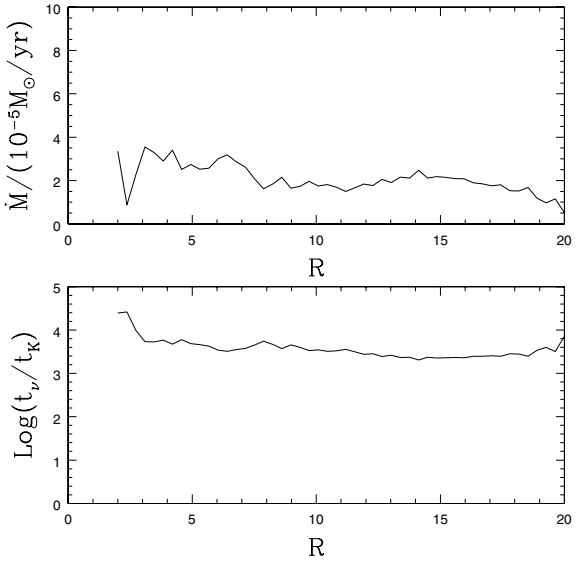

Figure 9. Bottom: Ratio of the accretion time-scale $t_\nu = \nu/R^2$ over the dynamical time-scale $t_{\rm K} = \Omega^{-1}$, for the $M_{\rm disc} = 0.5\,M_\star$ case. Top: Time-averaged mass accretion rate at the end of the simulation.

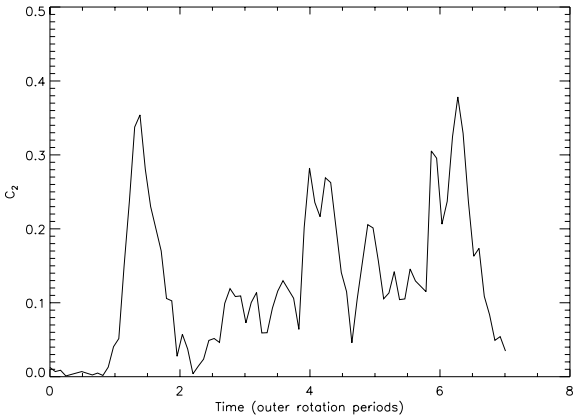

Figure 10. The $M_{\rm disc} = M_\star$ simulation. Amplitude of the $m = 2$ Fourier component of the disc surface density as a function of time. Major episodes of spiral activity can be recognized at $t \approx 1.5t_0$, $4t_0$ and $6t_0$.

It is interesting to compare the torque computed from equation (12), as shown in Fig. 13, with the expectations based on the linear modal theory of spiral structure in galaxy discs. The angular momentum flux associated with a given spiral mode can be computed based on the relevant wave action and group velocity (see Bertin 1983). We can thus express the angular momentum flux in terms of an effective α_m, associated with a mode with azimuthal wavenumber m. For a tightly wound mode in a light disc, we have

$$\alpha_m = \left|\frac{{\rm d}\ln\Omega}{{\rm d}\ln R}\right|^{-1} m\epsilon_0 \frac{2}{Q^2\hat{k}}\left(1 - \tfrac{1}{2}Q^2\hat{k}\right)|\Delta|^2, \qquad (15)$$

where $\Delta = \delta\Sigma_m/\Sigma$ is the amplitude of the mode, $\epsilon_0 = \pi G\,\Sigma/R\kappa^2$ and $\hat{k} = 2\epsilon_0 Rk$ is the dimensionless radial wavenumber of the mode. If we measure the amplitude Δ for the $m = 2$ spiral mode shown in the left panel of Fig. 11, and consider the short trailing branch of the dispersion relation, outside corotation we obtain $\alpha_{m=2} \approx 0.03$, which shows that a significant fraction of the angular momentum transport

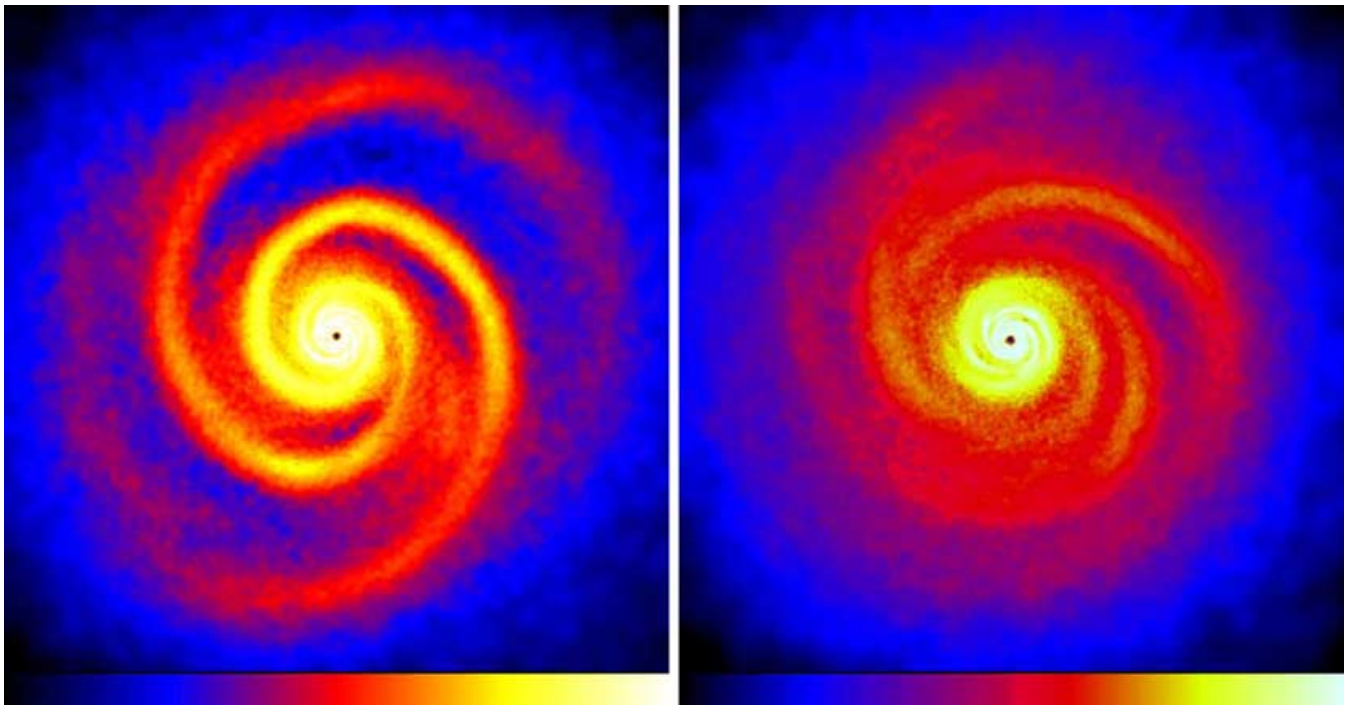

Figure 11. Surface density structure during the development of a spiral instability in the $M_{\rm disc} = M_\star$ case, at $t \approx 5.9 t_0$ (left) and at $t \approx 3 t_0$ (right). Both the density and the linear scales are the same as in Figs 1 and 5.

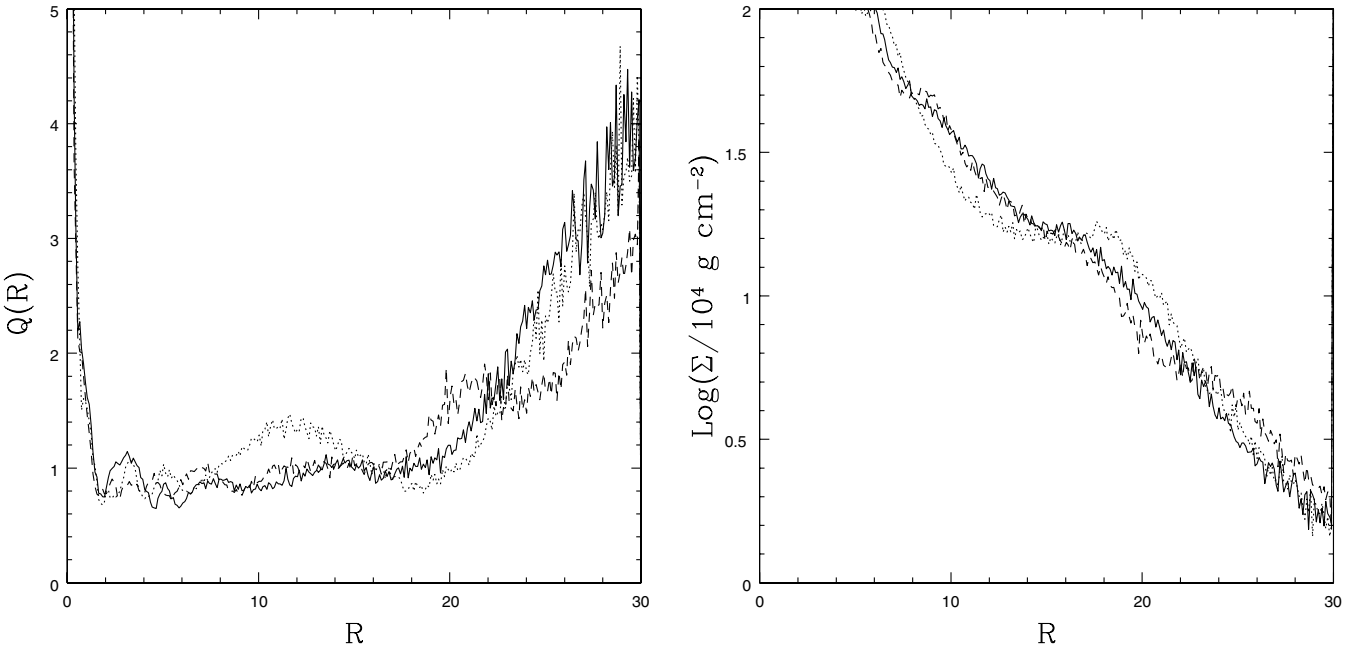

Figure 12. Evolution of Q (left) and of the azimuthally averaged surface density Σ (right) during the development of a spiral disturbance in the $M_{\rm disc} = M_\star$ case. The curves refer to $t \approx 5.4 t_0$ (before the onset of the instability; solid line), $t \approx 5.9 t_0$ (during the disturbance; dotted line), and $t \approx 6.3 t_0$ (after the spiral episode has vanished; dashed line).

is indeed associated with the global $m = 2$ mode. Of course, some effects beyond the simple linear theory for tightly wound modes in light discs, used in the above estimate, are expected (and should be further analysed) in the present case, in which the structure has reached non-linear amplitudes and develops in a relatively heavy disc.

An important question to be addressed is whether energy dissipation during the high spiral activity is intrinsically different to standard viscous dissipation, or, in other words, whether wave transport of energy is significant in our simulations. As discussed in Section 2, the test that we have generally used in order to assess this issue is a comparison between the value of α as computed from the

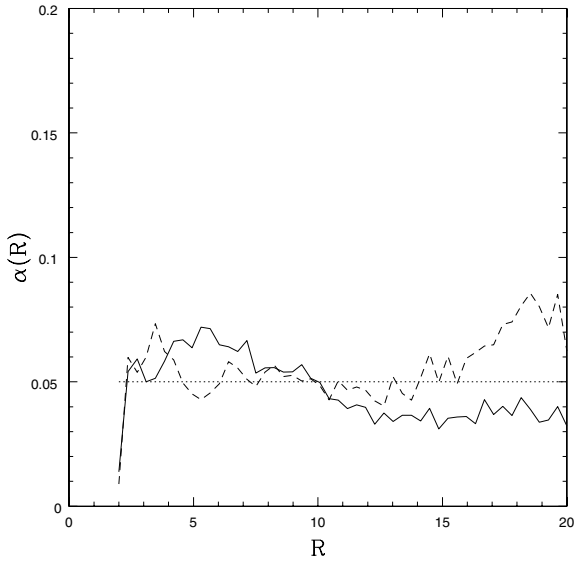

Figure 13. Time average of the effective α produced by gravitational instabilities between $t = 2.7t_0$ and $t = 3.5t_0$ (where no large-scale structure is observed; solid line) and between $t = 5.9t_0$ and $t = 6.6t_0$ (during the development of a large scale $m = 2$ disturbance; dashed line).

gravitational torque strength and the expected value obtained from a balance between viscous heating and cooling. In all simulations up to now we have interpreted the agreement between the two values as a demonstration that wave transport does not play a major role. In the present case, with $M_{\rm disc} = M_\star$, gravitational instabilities are clearly global and different in nature with respect to the lower-mass cases: here the pattern of the instability rapidly changes with time (in particular, the strength of the dominant $m = 2$ mode; see Fig. 10), and the value of Q, although always relatively close to unity, never really settles down in a self-regulated state. From Fig. 13 we see that, even during the high spiral activity, the value of α is relatively close to the expected value (dashed line in Fig. 13), being only slightly larger in the outer disc. It would be wrong, however, to interpret this small disagreement as an indication that wave energy transport is dominant, since the agreement is only expected if the disc is in thermal equilibrium. The change in internal energy of the disc as a result of the heating due to the development of the spiral can easily account for the discrepancy shown in Fig. 13.

These results do, however, suggest that massive discs never settle into a state of thermal equilibrium. If we interpret this in the same way as Laughlin et al. (1998), non-linear coupling between the different modes results in episodes when $m = 2$ modes heat the outer disc and make it more stable, followed by episodes when cooling dominates, and the disc is driven back towards a period of instability.

4 CONCLUSIONS

In this paper we have extended our previous analysis of the transport properties of self-gravitating discs, presented in Paper I. In particular, here we describe the results of two new simulations, in which the disc mass is of the same order of magnitude as the central object mass, namely $M_{\rm disc} = 0.5\,M_\star$ and $M_{\rm disc} = 1\,M_\star$. Given the specific region of the parameter space that we explore, our simulations have two previous analogues: the N-body simulations by Sellwood & Carlberg (1984), who mimicked the cooling of the stellar component of a galaxy disc through continuous accretion of stars; and a series of simulations by Laughlin et al. (Laughlin & Bodenheimer 1994; Laughlin, Korchagin & Adams 1997, 1998), who simulated a massive gaseous disc, adopting simple equations of state (mostly isothermal) without any specific cooling. The main difference between the latter simulations and those presented here lies in the way we handle the disc thermodynamics. In fact, we explicitly solve the energy equation of the disc, and introduce an external cooling term, simply parametrized in terms of a cooling time $t_{\rm cool} = \beta\Omega^{-1}$. By suitably choosing the parameter β, we are able to prevent the disc from fragmenting, and to produce a persistent spiral structure.

The specific aim of this work is to study the transport of angular momentum induced by gravitational instabilities and the associated energy dissipation process, to test in particular whether wave transport of energy plays an important role in the disc dynamics (Balbus & Papaloizou 1999). In this respect, the results of this paper can be summarized as follows:

(i) The development of a gravitational spiral structure is indeed able to transport angular momentum in the disc efficiently, hence favouring accretion. The time-averaged strength of the stress induced by the disc self-gravity, as measured by the parameter α (Shakura & Sunyaev 1973), is $\alpha \approx 0.05$, so that the associated energy dissipation [computed from equation (7)] almost balances the externally imposed cooling. This shows that global wave transport does not play a major role in our simulations, in line with the predictions of Balbus & Papaloizou (1999), who argued that self-regulated discs, with $Q \approx 1$ (as indeed are ours) should be free from wave transport effects.

(ii) Contrary to the results of Laughlin & Bodenheimer (1994), the accretion process induced by the disc self-gravity occurs on the long 'viscous' time-scale, rather than on the much shorter dynamical time-scale, so that a massive self-gravitating disc can survive for a relatively long period (see Fig. 9). This important difference can be understood by simply considering the parameter Q, as defined in equation (1). If Q is smaller than unity, gravitational instabilities develop and the disc responds so as to increase the value of Q to reach a stable configuration. If the disc is isothermal (as in Laughlin & Bodenheimer 1994), the only way this can be achieved is by significantly reducing Σ, i.e. by inducing a fast accretion process. On the other hand, if the disc is allowed to dissipate energy and to heat up, increasing the value of $c_{\rm s}$ (as in our simulations), the disc is stabilized more easily and the required amplitude of the gravitational disturbance is smaller, hence producing a slower accretion.

(iii) When the disc mass is small with respect to the central object, as in the case discussed in Paper I, the disc rapidly settles down in a self-regulated state where the amplitude of the spiral structure and the radial profile of Q change very little with time. In these cases, the spiral structure is tightly wound and dominated by high-m modes. In the case of high disc mass presented here, the evolution is more complex. In the case where $M_{\rm disc} = 0.5 M_\star$ we observe the development of an initial transient $m = 2$ spiral structure, which induces a strong redistribution of matter and a steepening of the surface density profile, before the disc is eventually able to settle down as in the low disc mass case. Similar initial transients are also observed by Mejia et al. (2005). We attribute it to an effect of the initial condition adopted. In particular, the chosen initial surface density profile $\Sigma \propto R^{-1}$ is actually shallower than analytical estimates of the surface density of self-regulated massive discs (Bertin & Lodato 1999). We have indeed shown that the initial transient steepens the surface

density profile in such a way that it matches the analytical estimates. The $M_{\rm disc} = 1\,M_\star$ case is even more complex: the disc never really settles down and it is self-regulated only in a time-averaged sense. The amplitude of the spiral disturbances changes strongly with time, and recurrent, short-lived, low-m spiral patterns develop in the disc (see Fig. 10). A similar behaviour has also been observed in the cooling simulations by Sellwood & Carlberg (1984) and Laughlin et al. (1998).

Another interesting result of our simulations is that, even at the high mass ratios considered here, they appear to be still consistent with the fragmentation criterion $t_{\rm cool} < 3\,\Omega^{-1}$. The above criterion had been previously tested either in local (Gammie 2001) or in global low disc mass simulations (Rice et al. 2003b). Even if the global simulations by Rice et al. (2003b) show that the actual threshold value for the cooling time is slightly increased with respect to the local estimates by Gammie (2001), we have shown here that, up to $M_{\rm disc} = 1\,M_\star$, the condition $t_{\rm cool} > 7.5\ \Omega^{-1}$ effectively prevents the fragmentation of the disc. In fact, note that, even if rather large density perturbations are experienced by the disc, especially during the initial transients, none of these density enhancements is long-lived. This is due primarily to our choice for the cooling time-scale and not to a limited resolution in our code. Indeed, simulations performed with the same number of particles as ours, but with a shorter cooling time, did show effective fragmentation (Rice et al. 2003b).

The present work completes the analysis described in Paper I, but can still be subject to many further refinements. In particular, all the results presented here and in Paper I are based on a specific form of the cooling term in the energy equation. On the other hand, as already mentioned, the outcome of gravitational instabilities in discs strongly depends on the assumptions about the disc thermal behaviour. Simulations that employ a cooling time constant with radius seem to show significant global energy transport (Mejia et al. 2005), in contrast to our results. Of course, both a constant cooling time-scale and our choice are highly idealized assumptions, and further studies are needed to assess which of the two is more reasonable. In principle, one could follow Johnson & Gammie (2003) and find a relation between cooling time and density, based on some opacity prescription. This would not, in general, give $t_{\rm cool}\Omega = $ constant. However, a cooling time proportional to the dynamical time-scale has the attractive feature of leading to a constant α, and since self-gravitating discs naturally evolve towards a self-regulated state, this might not be an unreasonable assumption (see also Bertin 1997).

Another important issue to be explored is how the disc response changes when different values for the ratio of the specific heats γ is used and whether this can affect the fragmentation criterion. Preliminary tests (Rice & Lodato, in preparation) seem to indicate that, when γ is decreased, the boundary cooling time for fragmentation increases. Actually, it might be more reasonable to express the fragmentation criterion in terms of a maximum gravitational stress sustainable by a non-fragmenting disc. Fig. 14 shows the relationship between α and $t_{\rm cool}$ implied by equation (9), for different values of γ. The horizontal dotted line indicates the value of α corresponding to $t_{\rm cool} = 3\,\Omega^{-1}$ when $\gamma = 2$ (the value adopted by Gammie 2001). In Paper I and here, we have shown that, when the disc does not fragment, the strength of the gravitational disturbances is such that equation (9) is approximately satisfied. If indeed there is a maximum α sustainable by a self-gravitating disc, then the disc would fragment whenever equation (9) implies a larger value of α. This would then be consistent with an increase of the limiting cooling time when γ is decreased (see Fig. 14). Further investigations are clearly needed to asses whether this is the case or not.

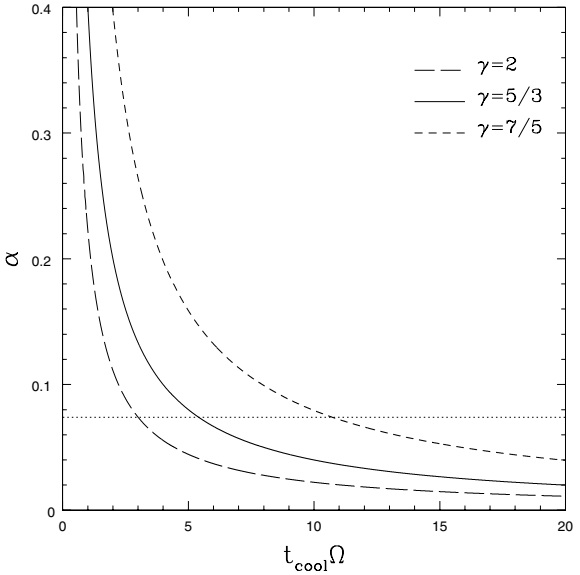

Figure 14. Relationship between α and $t_{\rm cool}$, described in equation (9), for different values of γ, namely: $\gamma = 2$ (long-dashed line), $\gamma = 5/3$ (solid line) and $\gamma = 7/5$ (short-dashed line). The dotted line indicates the value of α corresponding to $t_{\rm cool} = 3\,\Omega^{-1}$ in the case where $\gamma = 2$ (the value adopted by Gammie 2001).

ACKNOWLEDGMENTS

The simulations presented in this work were performed using the UK Astrophysical Fluid Facility (UKAFF). GL acknowledges support from the EU Research Training Network 'Young Stellar Clusters'. WKMR acknowledges support from a UKAFF Fellowship. We thank Phil Armitage, Giuseppe Bertin, Cathie Clarke and Jim Pringle for interesting and insightful discussions that significantly improved this paper.

REFERENCES

Armitage P. J., Livio M., Pringle J. E., 2001, MNRAS, 324, 705
Balbus S. A., Papaloizou J. C. B., 1999, ApJ, 521, 650
Balsara D. S., 1995, J. Comput. Phys., 121, 357
Bell K. R., Lin D. N. C., 1994, ApJ, 427, 987
Benz W., 1990, in Buchler J., ed., The Numerical Modeling of Nonlinear Stellar Pulsations. Kluwer, Dordrecht
Bertin G., 1983, A&A, 127, 145
Bertin G., 1997, ApJ, 478, L71
Bertin G., Lodato G., 1999, A&A, 350, 694
Boss A. P., 2002, ApJ, 576, 462
Boss A. P., 2004a, ApJ, 610, 456
Boss A. P., 2004b, ApJ, 616, 1265
Chini R., Hoffmeister V., Kimesvenger S., Neilbock M., Nürnberger D., Schmidtobreick L., Sterzik M., 2004, Nat, 429, 155
Gammie C. F., 2001, ApJ, 553, 174
Goodman J., Tan J. C., 2004, ApJ, 608, 108
Greenhill L. J., Gwinn C. R., 1997, Ap&SS, 248, 261
Haghighipour N., Boss A. P., 2003, ApJ, 583, 996
Huré J. M., 2000, A&A, 358, 378
Johnson B. M., Gammie C. F., 2003, ApJ, 597, 131

Kondratko P. T., Greenhill L. J., Moran J. M., Reid M. J., Menten K. M., Inoue M., 2005, ApJ, 618, 618
Larson R. B., 1984, MNRAS, 206, 197
Laughlin G., Bodenheimer P., 1994, ApJ, 436, 335
Laughlin G., Ròżyczka M., 1996, ApJ, 456, 279
Laughlin G., Korchagin V., Adams F. C., 1997, ApJ, 477, 446
Laughlin G., Korchagin V., Adams F. C., 1998, ApJ, 504, 945
Launhardt R., Sargent A. I., 2001, ApJ, 562, 173
Lin D. N. C., Pringle J. E., 1987, MNRAS, 225, 607
Lodato G., Bertin G., 2003a, A&A, 398, 517
Lodato G., Bertin G., 2003b, A&A, 408, 1015
Lodato G., Rice W. K. M., 2004, MNRAS, 351, 630 (Paper I)
Lynden-Bell D., Kalnajs A. J., 1972, MNRAS, 157, 1
Mejia A. C., Durisen R. H., Pickett M. K., Cai K., 2005, ApJ, 619, 1098
Monaghan J. J., 1992, ARA&A, 30, 543
Natta A., Testi L., Neri R., Shepherd D. S., Wilner D. J., 2004, A&A, 416, 179
Nelson A. F., Benz W., Ruzmaikana T. V., 2000, ApJ, 529, 357
Paczyński B., 1978, Acta Astron., 28, 91
Pickett B. K., Cassen P., Durisen R. H., Link R., 1998, ApJ, 504, 468
Pickett B. K., Cassen P., Durisen R. H., Link R., 2000, ApJ, 529, 1034
Pickett B. K., Mejia A. C., Durisen R. H., Cassen P. M., Berry D. K., Link R. P., 2003, ApJ, 590, 1060
Pringle J. E., 1981, ARA&A, 19, 137
Rice W. K. M., Armitage P. J., Bate M. R., Bonnell I. A., 2003a, MNRAS, 338, 227
Rice W. K. M., Armitage P. J., Bate M. R., Bonnell I. A., 2003b, MNRAS, 339, 1025
Rice W. K. M., Armitage P. J., Bate M. R., Bonnell I. A., Jeffers S. V., Vine S. G., 2003c, MNRAS, 346, L36
Rice W. K. M., Lodato G., Pringle J. E., Armitage P. J., Bonnell I. A., 2004, MNRAS, 355, 543
Sellwood J. A., Carlberg R. G., 1984, ApJ, 282, 61
Shakura N. I., Sunyaev R. A., 1973, A&A, 24, 337

This paper has been typeset from a TEX/LATEX file prepared by the author.